ABSTRACT

PARHIZI, SINA. Impact of Wind Power Integration on Power System Oscillations. (Under the direction of Dr. Aranya Chakrabortty).

It is increasingly becoming critical to understand how injection of large-scale wind power affects the dynamic oscillations in the grid especially the low frequency inter-area oscillations, as wind penetration continues to increase in the North American grid. Objective of this thesis is to analytically investigate the integration of wind power penetration with oscillation dynamics of the grid, and to carry out several test cases to study how various wind farm layouts and their corresponding fluid dynamical properties impact the frequency of the oscillation modes, especially the inter-area modes. In this work, an equivalent model for a wind farm was developed, which allows to study different layouts and their impact on power systems. It was observed that DFIG integration results in the modes associated with DFIG to be negative real and having no oscillatory behavior. Impact of changes in layout of the wind farm connected to the grid on its oscillations is studied.

Impact of Wind Power Integration on Power System Oscillations

by
Sina Parhizi

A thesis submitted to the Graduate Faculty of
North Carolina State University
in partial fulfillment of the
requirements for the degree of
Master of Science

Electrical Engineering

Raleigh, North Carolina

2013

APPROVED BY:

Dr. Aranya Chakrabortty Committee Chair	Dr. Mesut Baran

Dr. Subhashish Bhattacharya

DEDICATION

To my grandparents

and

my parents

ACKNOWLEDGMENTS

I acknowledge great support and help of my dear advisor Dr. Aranya Chakrabortty. I express my gratitude to my committee members Dr. Baran and Dr. Bhattacharya.

I thank my parents for their love, encouragement and inspiration.

TABLE OF CONTENTS

LIST OF TABLES

LIST OF FIGURES

CHAPTER 1

Introduction

The global need for clean sustainable energy has driven the power systems research to study problems arising from the wind power systems integration in the grid [1], [2] This trend is mostly involved with issues regarding stochasticity of wind speeds and its impact on steady state and financial aspects [3], [4] of the power system. A large part of these studies focus on wind farm integration in distribution level and integration of distributed wind energy generation in the medium-voltage level [5], where it is tried to smooth the distributed generation output using energy storage [6], their placement and voltage stability [7]. Another way of wind integration is large-scale integration of large wind farms. This approach is especially applicable to cases where wind generation and demand locations are far from each other [8].

There have not been much studies on wind farm behavior in the power systems and its impact on the power system dynamics compared to their steady state behavior and economic concerns. Impact of distributed wind generation on the system transient stability was studied in [9]. For the case of large-scale integration, it is necessary to obtain an equivalent model of a farm composed of tens of turbine-generators to reduce computation complexity [10]. Due to the structure of wind generators, it is required to develop a special model for them which is different inherently from the conventional synchronous generators [11], [12], [13].

The distinct physical nature of synchronous generators, where its mechanical speed is synchronous to its stator voltage frequency, causes oscillations in the power systems. In a wind turbine generator, which is represented by a Doubly-Fed Induction Generator (DFIG) there are no such relationships between rotor speed and electrical frequency in these asynchronous generators.

The synchronous generators are modeled as a voltage source behind a transient reactance where the phase angle of the voltage source is the angle between its rotor and synchronous reference frame. DFIG can be modeled as a current source whose power output is only dependent on wind speed and rotor speed, and the bus it is connected to, is treated as a PQ bus [14].

Some work has been done to study dynamic impacts of wind power namely [15] and by NREL in [16] but mostly at turbine level and not grid level. It is increasingly becoming critical to understand how injection of large-scale wind power affects the dynamic oscillations in the grid especially the low frequency inter-area oscillations, as wind penetration continues to increase in the North American grid. For example, recent studies in the New York Power Authority (NYPA) has shown that fluctuations in the operating conditions in the wind farms located at Altona and Chateaguay substations in upstate New York and Canada can cause severe oscillations in the Marcy substation close to New York City, which is connected to the wind farms directly by a 345 KV transmission line.

Objective of this thesis is to analytically investigate the integration of wind power penetration with oscillation dynamics of the grid, and to carry out several test cases to study how various wind farm layouts and their corresponding fluid dynamical properties impact the frequency of the oscillation modes, especially the inter-area modes.

In this work, an equivalent model for a wind farm was developed, which allows to study different layouts and their impact on power systems. It was observed that DFIG integration results in the modes associated with DFIG to be negative real and having no oscillatory behavior. Impact of changes in layout of the wind farm connected to the grid on its oscillations is studied.

This thesis is presented in three chapters. In chapter two, model of the turbine-generator is derived and its coupling with the grid swing dynamics is shown. In chapter 3, an equivalent model using system identification is discussed. In chapter 4, another equivalent model is presented and applied to different wind farm layouts.

CHAPTER 2

Wind turbine-generator integrated power system modeling

A system of a DFIG and a synchronous generator (SG) is considered. The synchronous generator is modeled using a classic model of voltage source behind a reactance equivalent to sum of line and transient reactance. For the DFIG a model used in [17] is used. The load is constant.

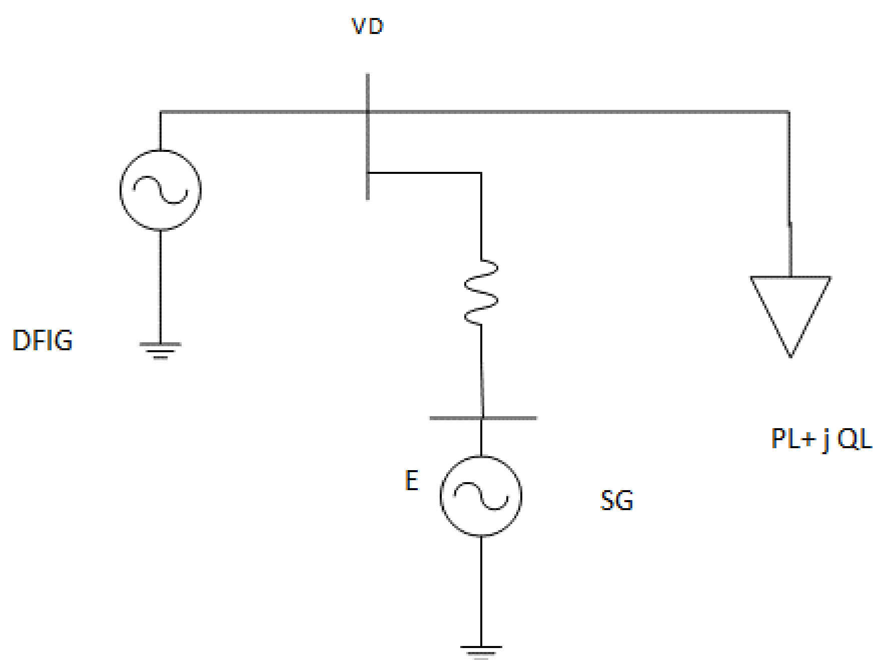

Figure 1- System studied in this work

A doubly fed induction generator is used as the wind generator. A single mass model is considered, so there is no twist in the turbine rotor shaft.

2.1 Wind Turbine

The mechanical power output of the wind turbine is

$$P_m = \frac{1}{2}\rho A C_p v_w^3 \ \text{[W]} \quad (2.1)$$

Where ρ is the air density, A is the area turbine blade sweeps, C_p is the efficiency coefficient dependent on pitch angle, rotor speed and wind speed. Assuming an ideal rotor speed control so that turbine always operates at maximum power, C_p is always a constant equal to its maximum value.

The mechanical torque is obtained in per unit to be used in the equation of motion:

$$T_m = \frac{\frac{1}{2}\rho A C_p v_w^3}{\omega_r} \ \text{[N.m]} \ (2.2)$$

In per unit:

$$T_m = \frac{1}{2}\frac{\rho A \omega_b C_p v_w^3}{S_b \omega_r} = k\frac{v_w^3}{\omega_r} \ \text{[p.u]} \ (2.3)$$

2.2 Doubly Fed Induction generator

Doubly Fed Induction generator (DFIG) electrical variables are expressed in synchronous reference frame, so DFIG output current phasor, I_D, can be written in this way (See figure 2):

$$\overline{I_D} = I_{qs} - jI_{ds} \quad (2.4)$$

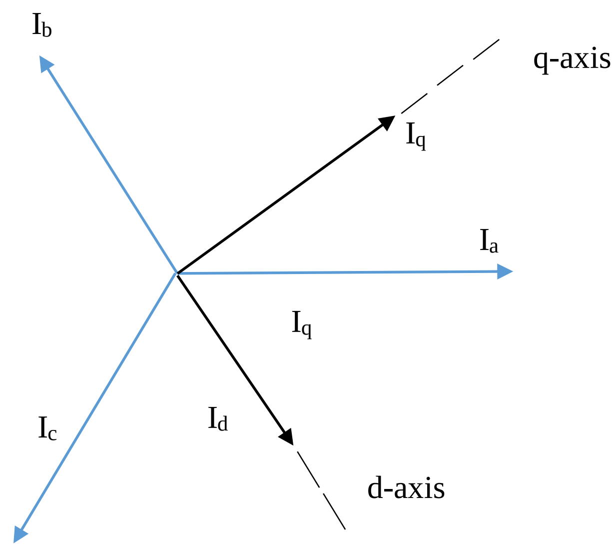

Figure 2- stator current vector decomposition in dq-rotating reference frame

The DFIG dynamic model can be written as [17]:

$$\frac{d\varphi_{qs}}{dt} = V_{qs} + R_s I_{qs} - \varphi_{ds} \qquad (2.4)$$

$$\frac{d\varphi_{ds}}{dt} = V_{ds} + R_s I_{ds} - \varphi_{qs} \qquad (2.5)$$

$$\frac{1}{\omega_s}\frac{d\varphi_{qr}}{dt} = V_{qr} - R_r I_{qr} - \frac{(\omega_s - \omega_r)}{\omega_s}\varphi_{dr} \qquad (2.6)$$

$$\frac{1}{\omega_s}\frac{d\varphi_{dr}}{dt} = V_{dr} - R_r I_{qr} - \frac{(\omega_s - \omega_r)}{\omega_s}\varphi_{qr} \qquad (2.7)$$

Where flux linkages can be written in terms of the rotor and stator currents:

$$\varphi_{qr} = -X_m I_{qs} + X_r I_{qr} \qquad (2.8)$$

$$\varphi_{dr} = -X_m I_{ds} + X_r I_{dr} \qquad (2.9)$$

$$\varphi_{qs} = -X_s I_{qs} + X_m I_{qr} \qquad (2.10)$$

$$\varphi_{ds} = -X_s I_{ds} + X_m I_{dr} \qquad (2.11)$$

Doubly fed induction generator is a wound-rotor asynchronous generator where rotor current can be controlled to achieve speed control [18]. The 5th order dynamic model is considered to model the doubly-fed induction generator in this study. In this model, stator and rotor flux linkage dynamics are considered to be too fast and generator variables are considered to be algebraic. Studies in [17] show that this is a valid assumption since flux linkage dynamics time constants is small compared to other dynamics. Consequently using the above equations and setting flux linkage dynamics to zero, stator and rotor voltages can be written in terms of rotor and stator currents.

$$V_{qs} = -R_s I_{qs} - X_s I_{ds} + X_m I_{dr} \qquad (2.12)$$

$$V_{ds} = -R_s I_{ds} - X_s I_{qs} - X_m I_{qr} \qquad (2.13)$$

$$V_{qr} = R_r I_{qr} - s X_m I_{ds} + s X_r I_{dr} \qquad (2.14)$$

$$V_{dr} = R_r I_{dr} + s X_m I_{qs} + s X_r I_{qr} \qquad (2.15)$$

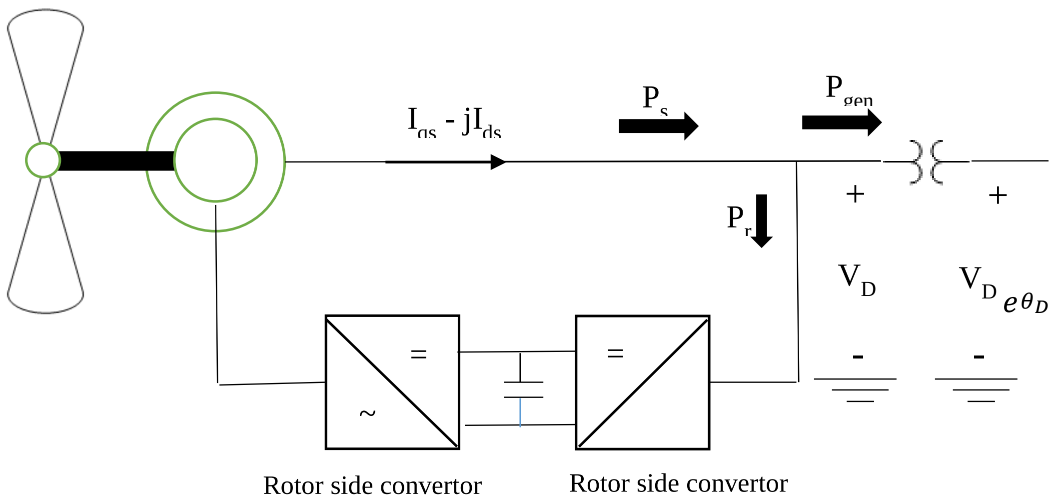

Figure 3- Power flow in the DFIG

Using a fast vector control to decouple active and reactive power control, d-axis is aligned with the stator flux axis so that $V_{ds}=0$ and $V_{qs}=V_D$. DFIG terminal angle is kept equal to zero using am ideal shift-angle transformer. DFIG terminal voltage is obtained from running power flow, treating that bus as a PQ bus, the DFIG power is injected to it.

We can write these relations for the DFIG stator output power:

$$S_{SD}=V_D I_D^*=V_D(I_{qs}+jI_{ds}) \qquad (2.16)$$

Rotor reactive power output reference is zero so rotor power is equal to $V_{dr}I_{dr}+V_{qr}I_{qr}$ which is added to the stator power. In summary this can be stated:

$$P_{gen} = P_s - P_r = V_D I_{qs} - (V_{qr} I_{qr} + V_{dr} I_{dr}) \qquad (2.17)$$

$$Q_{gen} = V_D I_{ds} \qquad (2.18)$$

The electrical torque can be written as

$$T_e = \varphi_{dr} I_{qr} - \varphi_{dr} I_{qr} \qquad (2.19)$$

Using equations derived for flux linkages in terms of current it can be written as:

$$T_e = X_m (I_{qs} I_{dr} - I_{ds} I_{qr}) \qquad (2.20)$$

2.3 Power controllers

In a DFIG rotor is connected to the grid through a grid-side convertor as shown in Figure 3. The grid side converter is modeled as a controlled current source and the rotor side as a controlled voltage source. and a rotor-side convertor PI-controllers are used to control active and reactive power, modeled as expressed in figure 3.

The following dynamic equations are obtained from the controllers:

$$\frac{d x_1}{dt} = K_{I1} [P_{ref} - P_{gen}] \qquad (2.21)$$

$$\frac{d x_2}{dt} = K_{I2} [K_{P1} (P_{ref} - P_{gen}) + x_1 - I_{qr}] \qquad (2.22)$$

$$\frac{d\,x_3}{dt} = K_{I3}\,[Q_{ref} - Q_{gen}] \qquad (2.23)$$

$$\frac{d\,x_4}{dt} = K_{I4}\,[K_{P3}\,(Q_{ref} - Q_{gen}) + x_3 - I_{dr}] \qquad (2.24)$$

And algebraic equations:

$$V_{qr} = K_{P2}\,[K_{P1}\,(P_{ref} - P_{gen}) + x_1 - I_{qr}] + x_2 \qquad (2.25)$$

$$V_{dr} = K_{P4}\,[K_{P3}\,(Q_{ref} - Q_{gen}) + x_3 - I_{dr}] + x_4 \qquad (2.26)$$

It is assumed that the wind speed is between cut-in and rated speeds so the turbine operates on an optimal curve as the active power reference defined by $P_{ref} = C\omega r^3$. The reactive power reference is set to a constant value.

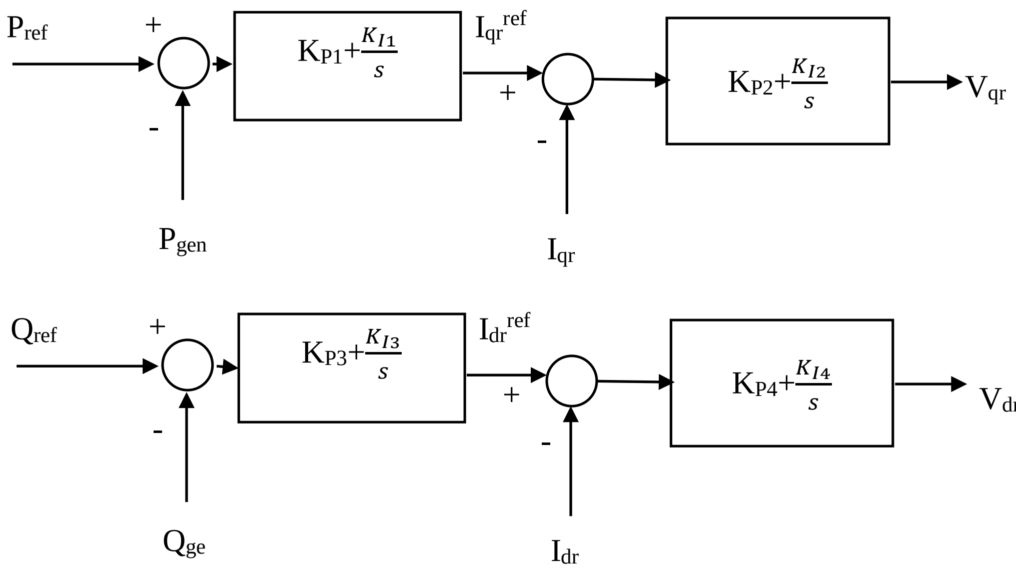

Figure 4- Active and reactive power controllers

In order to obtain the DFIG bus voltage, Network algebraic equations are written by Kirchhoff's law in the form of power

$$\frac{E\,V_D}{X}\sin\,(\delta-\theta_D)+P_{gen}\;=P_L \qquad (2.27)$$

$$\frac{E\;V_D\;\cos\,(\delta-\theta_D)-V_D{}^{2}}{X_d}+Q_{gen}\;=\;Q_L \qquad (2.28)$$

Where P_L, Q_L are constant values representing active and reactive powers of the load connected to the bus.

Assuming a single-mass model for the turbine-generator using (2.3) and (2.20) we can write the equation of motion as:

$$\frac{d\omega_r}{dt} = \frac{\omega_s}{2\,HD}\ [\ T_m - x_m\ I_{qs}\ I_{dr} + X_m\ I_{ds}\ I_{qr}\ ] \qquad (2.29)$$

2.4 DFIG dynamic algebraic equations

The set of algebraic dynamic variables can be summarized as below:

$$\frac{d\omega_r}{dt} = \frac{\omega_s}{2\,HD}\ [\ T_m - x_m\ I_{qs}\ I_{dr} + X_m\ I_{ds}\ I_{qr}\ ]$$

$$\frac{d\,x_1}{dt} = K_{I1}\ [P_{ref} - P_{gen}]$$

$$\frac{d\,x_2}{dt} = K_{I2}\ [K_{P1}\ (P_{ref} - P_{gen}) + x_1 - I_{qr}]$$

$$\frac{d\,x_3}{dt} = K_{I3}\ [Q_{ref} - Q_{gen}]$$

$$\frac{d\,x_4}{dt} = K_{I4}\ [K_{P3}\ (Q_{ref} - Q_{gen}) + x_3 - I_{dr}]$$

SG dynamic variables:

$$\frac{d\theta}{dt} = \omega - \omega_s$$

$$\frac{2\,H}{\omega_s}\ \frac{d\omega}{dt} = P_m - \frac{V\,V_D}{X1}\,\mathrm{Sin}\,(\theta - \theta_D)$$

DFIG algebraic variables include:

$$0 = -V_{qr} + K_{P2}\,[K_{P1}\,(P_{ref} - P_{gen}) + x_1 - I_{qr}] + x_2$$

$$0 = -V_{dr} + K_{P4}\,[K_{P3}\,(Q_{ref} - Q_{gen}) + x_3 - I_{dr}] + x_4$$

$$0 = -V_D - R_s\,I_{qs} - X_s\,I_{ds} + X_m\,I_{dr}$$

$$0 = -R_s\,I_{ds} - X_s\,I_{qs} - X_m\,I_{qr}$$

Where V_{qr} and V_{dr} are obtained from DFIG rotor algebraic variables:

$$V_{qr} = R_r\,I_{qr} - s\,X_m\,I_{ds} + s\,X_r\,I_{dr}$$

$$V_{dr} = R_r\,I_{dr} + s\,X_m\,I_{qs} + s\,X_r\,I_{qr}$$

where slip is defined:

$$s = \frac{\omega_s - \omega_r}{\omega_s}.$$

And:

$$P_{gen} = V_D I_{qs} - (V_{qr}\,I_{qr} + V_{dr}\,I_{dr})$$

$$Q_{gen} = V_D I_{ds}$$

$$T_m = B\,\omega_s\,C_P\,\frac{v_w^3}{\omega_r}$$

$$P_{ref} = C\,\omega_r^3$$

$$Q_{ref} = 0$$

2.5 Linearization

The system is modeled by the set of differential algebraic equations (DAE):

$$\dot{X} = f\ (X, Y, u) \qquad (2.29)$$

$$0 = g\ (X, Y). \qquad (2.30)$$

Linearizing the nonlinear DAE around an equilibrium point (X_0, Y_0):

$$\Delta\dot{X} = A\ \Delta X + B\ \Delta Y + \Delta U \qquad (2.31)$$

$$0 = C\ \Delta X + D\ \Delta Y \qquad (2.32)$$

Then we use Kron's reduction:

$$\Delta\dot{X} = (A - BD^{-1}C)\ \Delta X + \Delta U = A_{sys}\ \Delta X + \Delta U \qquad (2.33)$$

We are interested in studying the characteristics of A_{sys} [19]. States of DFIG and synchronous generator are named as Δx_D and Δx_S, respectively. Assuming zero input we obtain:

$$\begin{bmatrix} \Delta\dot{x}_D \\ \Delta\dot{x}_S \end{bmatrix} = \begin{bmatrix} M & 0 \\ P & Q \end{bmatrix} \begin{bmatrix} \Delta x_D \\ \Delta x_S \end{bmatrix} \qquad (2.34)$$

$$\Delta\dot{x}_S = Q\ \Delta x_S + P\ \Delta x_D = Q\ \Delta x_S + P\ (e^{Mt}\Delta x_{D0}) \quad (2.35)$$

Where A matrix is:

$$\begin{bmatrix} \frac{\omega_s}{2H_D}(-\frac{kv_w^3}{\omega_r^2}) & 0 & 0 & 0 & 0 & 0 & 0 \\ 3K_{I1}C\omega_r^3 & 0 & 0 & 0 & 0 & 0 & 0 \\ 3K_{I1}K_{P1}C\omega_r^3 & K_{I2} & 0 & 0 & 0 & 0 & 0 \\ 0 & 0 & 0 & 0 & 0 & 0 & 0 \\ 0 & 0 & 3K_{I4} & 0 & 0 & 0 & 0 \\ 0 & 0 & 0 & 0 & 0 & 0 & 1 \\ 0 & 0 & 0 & 0 & 0 & -\frac{\omega_s}{2H_D}\frac{EV_D}{X}\cos\ (\delta-\theta) & 0 \end{bmatrix}_{X_0, Y_0}$$

And B matrix is:

$$\begin{bmatrix} \frac{\omega_s}{2H_D}X_m I_{qr} & -\frac{\omega_s}{2H_D}X_m I_{dr} & -\frac{\omega_s}{2H_D}X_m I_{qs} & -\frac{\omega_s}{2H_D}X_m I_{ds} & 0 & 0 & 0 & 0 \\ 0 & 0 & 0 & 0 & 0 & 0 & -K_{I1} & 0 \\ 0 & 0 & 0 & -K_{I2} & 0 & 0 & -K_{I2}K_{P2} & 0 \\ 0 & 0 & 0 & 0 & 0 & 0 & 0 & -K_{I3} \\ 0 & 0 & -K_{I4} & 0 & 0 & 0 & 0 & -K_{I4}K_{P4} \\ 0 & 0 & 0 & 0 & 0 & 0 & 0 & 0 \\ 0 & 0 & 0 & 0 & \frac{\omega_s}{2H_D}\frac{E}{X}\sin(\delta-\theta) & -\frac{\omega_s}{2H_D}\frac{EV_D}{X}\cos\ (\delta-\theta) & 0 & 0 \end{bmatrix}_{X_0, Y_0}$$

C matrix is:

$$\begin{bmatrix} \frac{X_r I_{dr} - X_m I_{dr}}{\omega_s} + 3C\omega_r^2 & 1 & 1 & 0 & 0 & 0 & 0 \\ \frac{X_r I_{qr} + X_m I_{qs}}{\omega_s} & 0 & 0 & 1 & 1 & 0 & 0 \\ 0 & 0 & 0 & 0 & 0 & 0 & 0 \\ 0 & 0 & 0 & 0 & 0 & 0 & 0 \\ 0 & 0 & 0 & 0 & 0 & \frac{EV_D}{X}\cos(\delta-\theta) & 0 \\ 0 & 0 & 0 & 0 & 0 & 0 & 0 \\ 0 & 0 & 0 & 0 & 0 & 0 & 0 \\ \frac{I_{dr}(X_r I_{qr} + X_m I_{qs}) + I_{qr}(X_r I_{dr} + X_m I_{ds})}{\omega_s} & 0 & 0 & 0 & 0 & 0 & 0 \end{bmatrix}_{X_0, Y_0}$$

D matrix is:

$$\begin{bmatrix} sX_m & 0 & -sX_r & R_r - K_{1P} & 0 & K^2_{1P} & 0 & 0 \\ 0 & -sX_m & -R_r - K_{2P} & -sX_r & 0 & 0 & 0 & -K^2_{2P} \\ -X_s & -R_s & X_m & 0 & -1 & 0 & 0 & 0 \\ -R_s & X_s & 0 & 0 & -X_m & 0 & 0 & 0 \\ 0 & 0 & 0 & 0 & \frac{E\sin(\delta-\theta)}{X} & -\frac{V_D}{X}\cos(\delta-\theta) & 1 & 0 \\ 0 & 0 & 0 & 0 & \frac{E\cos(\delta-\theta) - 2V_D}{X} & 0 & 0 & 1 \\ V_D & 0 & 0 & 0 & I_{ds} & 0 & 0 & -1 \\ -sX_m I_{qr} & V_D - sX_m I_{ds} & -(V_{dr} + R_r I_{dr} + sX_r I_{qr}) & -(V_{qr} + R_r I_{qr} + sX_r I_{dr}) & I_{qs} & 0 & -1 & 0 \end{bmatrix}_{X_0, Y_0}$$

Table 1- Impact of wind speed on imaginary part of the synch. gen complex poles at different inertias

Wind Speed (m/s)	*H=5s*	*H=10s*	*H=30s*
10	6.4637	4.5704	2.6384
20	6.4580	4.5664	2.6361
30	6.4035	4.5278	2.6138

2.6 Simulations

Impact of changing different wind farm factors on synchronous generator speed and imaginary part of A_{sys} eigenvalues is studied in Table 1 and figure 4.

The system consisting of one DFIG and one synchronous generator is considered, and imaginary part of its complex poles are calculated at different inertias and wind speed levels. This data is shown in Table 1. It is observed that when wind speed changes the percent change of imaginary poles at different inertias are almost equal. Figure 4, shows speed, omega, in terms of time of the same synchronous generator at different wind speeds.

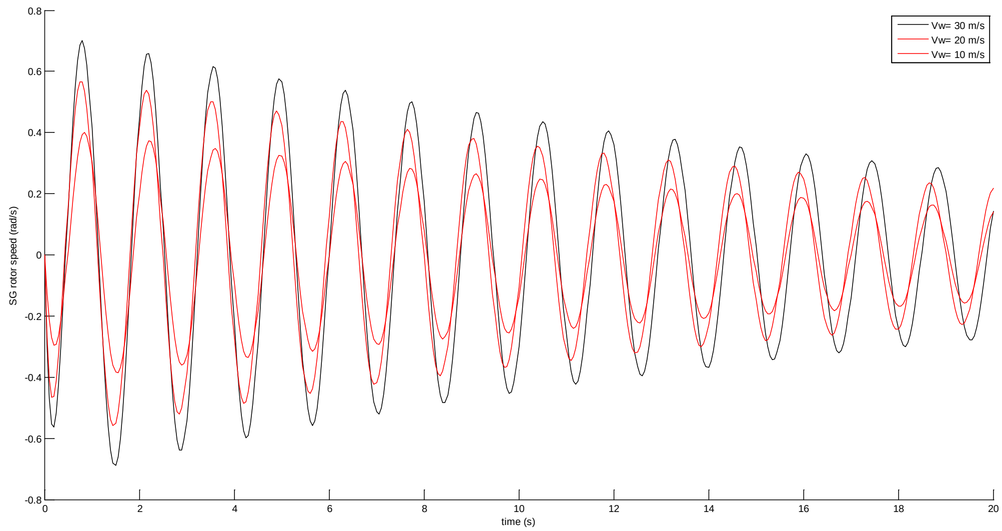

time (s)

Figure 5-Impulse response of a synchronous. Generator with inertia H= 10 s when connected to a DFIG operating at different wind speeds: 10m/s, 20 m/s and 30 m/s

CHAPTER 3

Equivalent model of a wind farm

The wind farm modeled in the previous chapter consisted of only one turbine-generator. Actually the wind farms are normally composed of more than one generator patterned in different layouts depending on the farm site terrain features. This chapter discusses modeling farms composed of more than one turbine-generator.

3.1 Wake effect

Wind speed and consequently the generated powers of generators at different locations in a farm are not equal. The wind speed decreases as wind passes through a turbine and some of its energy is transferred to it.

This phenomenon of reduction of wind speed behind a wind turbine is called Wake effect. Using the wake effect relationship in [20], U_x, the wind speed behind a wind turbine at distance X can be obtained [21] [22].

$$U_x = U_0\left(1 - \frac{1-\sqrt{1-C_T}}{(1+2k\frac{X}{D})^2}\right) \qquad (3.1)$$

Where X is distance behind the turbine, U_x is the wind speed at distance X, U_0 is the initial wind speed being applied to the turbine. Is thrust coefficient, k is wake effect constant considered equal to 0.11, and D is diameter of the wind turbine. (See figure 5).

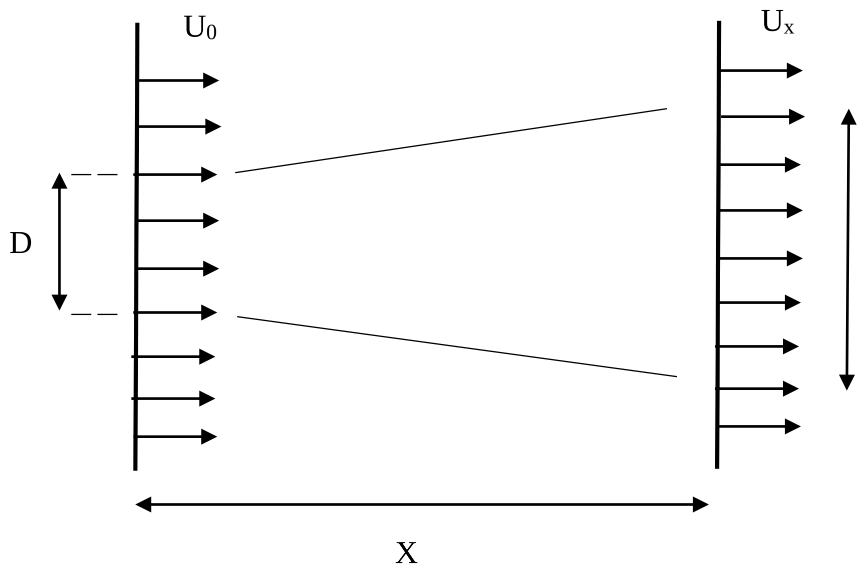

Figure 6- Wake effect

3.2 System identification

Two approaches were used to obtain an equivalent model of a wind farm: System identification and aggregation. In system identification approach, the detailed farm order is reduced to one single DFIG, and the parameters of this equivalent model are found by input-output identification. Sums of input powers and output powers are considered as inputs and outputs of the equivalent system. Using batch least squares, the z-domain transfer function coefficients are obtained. The transfer function is then computed in the s-domain.

$$\Delta \dot{x}_S = Q\ \Delta x_S + P\ \Delta u \quad (3.2)$$

$$\Delta y = L \Delta x \quad (3.3)$$

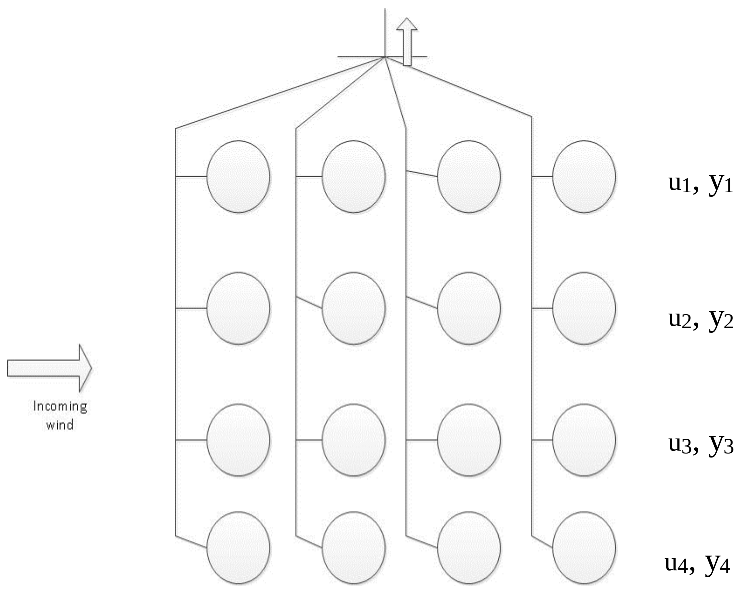

Figure 7- Using Inputs and outputs of DFIGs in a farm for system identification

The transfer function, G(s), is obtained:

$$G(s) = \frac{Y(s)}{U(s)} = L\ (sI - Q)^{-1}\ P \quad (3.4)$$

Transferring it to the z-domain we obtain:

$$G(z)=\frac{Y(z)}{U(z)}=\frac{a_0+a_1z^{-1}+\cdots+a_mz^{-m}}{1+b_1z^{-1}+\cdots+b_nz^{-n}} \quad (3.5)$$

So in time domain it can be written that:

$$y(k)=a_0u(k)+a_1u(k-1)+\cdots+a_mu(k-m)-(b_1y(k-1)+\cdots+b_ny(k-n)) \quad (3.6)$$

$$y(k)=\begin{bmatrix} y(k\text{-}1) & y(k\text{-}2) & \ldots & y(k\text{-}n) & u(k) & u(k\text{-}1) & \ldots & u(k\text{-}m) \end{bmatrix}\begin{bmatrix} b_1 \\ b_2 \\ \vdots \\ b_n \\ a_0 \\ a_1 \\ \vdots \\ a_m \end{bmatrix} \quad (3.7)$$

$$\Rightarrow Y=\Phi\theta \quad (3.8)$$

Where Φ is the Regressor and includes input and output data from time prior to k, and θ is the vector of unknown parameters. In this way the transfer function of the system can be obtained. This method is useful in cases like [23] where actual parameters of the system are not needed, but in this study we need to have the system parameters, so we use another approach which is presented later.

CHAPTER 4

Wind farm modeling and simulation

The method proposed in [24] is used to find the equivalent model of a large wind farm is aggregation of the turbine generators. The wind farm is approximated with one turbine generator which total mechanical power of the farm is applied to it. All the DFIGs in the farm are considered identical and connected in parallel to the point of common coupling (PCC). The structure of the equivalent model is considered to be similar to each of the DFIGs but with different parameters. The equivalent model is desired to possess dynamic and fault current behavior close to the actual farm.

The parameters of the model are found by the aggregation method used in [24], [17]. The power and currents, x_1^{eq} and x_3^{eq} of the aggregated model are Ng times higher than each single DFIG, where Ng is the total number of generators in the farm. The voltages and speed of the model is at the same order as each single DFIG.

An equivalent wind speed is defined, which applying it to the equivalent model would result in the same total mechanical power of the whole farm:

$$v_w^e = \sqrt[3]{\frac{\sum_{i=1}^{Ng} v_{w,i}^3}{Ng}} \qquad (4.1)$$

$$P_m^e = \frac{1}{2}\rho A \omega_b C_p \sum_{i=1}^{Ng} v_{w,i}^3 \qquad (4.2)$$

So it can be written

$$P_m^e = \rho A \omega_b C_p^e v_m^{e\ 3} \quad (4.3)$$

Using the aggregation method, the equivalent model parameters changing compares to one turbine generators are found as below:

$$K_{p2}{}^{eq} = \frac{Kp2}{Ng} \qquad K_{p4}{}^{eq} = \frac{Kp4}{Ng}$$

$$K_{I2}{}^{eq} = \frac{KI2}{Ng} \qquad K_{I4}{}^{eq} = \frac{KI4}{Ng}$$

$$X_m{}^{eq} = \frac{Xm}{Ng} \qquad X_r{}^{eq} = \frac{Xr}{Ng}$$

$$X_m{}^{eq} = \frac{Xm}{Ng} \qquad X_r{}^{eq} = \frac{Xr}{Ng}$$

$$X_s{}^{eq} = \frac{Xs}{Ng} \qquad R_s{}^{eq} = \frac{Rs}{Ng}$$

Parameters not mentioned here remain the same as for one turbine generator.

4.1 Simulations

Various layouts are studied to see their impact on oscillations. In figure 7, two different layouts of four identical generators are considered. In case A, the four generators are set in a line parallel to the direction of the wind blow, and every two consecutive rows are distanced 120 meters from each other. In case B, the four generators are set in two rows and two columns. Speeds of the synchronous generator in the two cases are presented in figure 8. Frequencies of the two cases differ, as the imaginary parts of the complex eigenvalues are 7.73 and 7.44 for cases A and B, respectively.

Increasing number of generators more than a limit results in creating unstable poles. For example, when there is one column of turbines parallel to the wind direction, increasing the number of rows more than 5, will cause a positive real pole.

Table 2- Change in eigenvalue imaginary part in different operatinal conditions

Number	*# of rows*	*# of columns*	*Space between rows*	*Imaginary part of complex eigenvalues*	*Wind speed*
1	1	6	200	7.8653	14
2	6	1	200	8.7728	14
3	6	1	100	8.9980	14

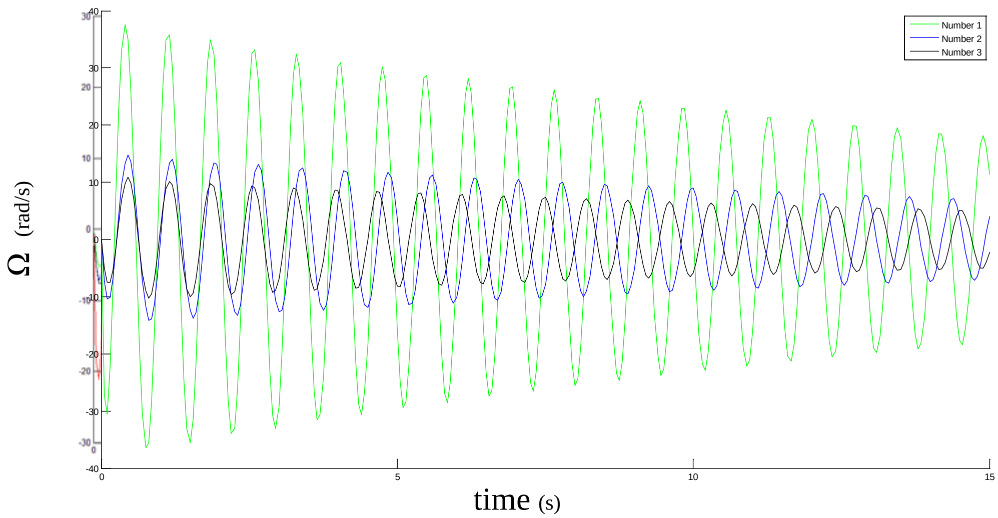

Figure 8- Impulse response of different conditions in Table 2

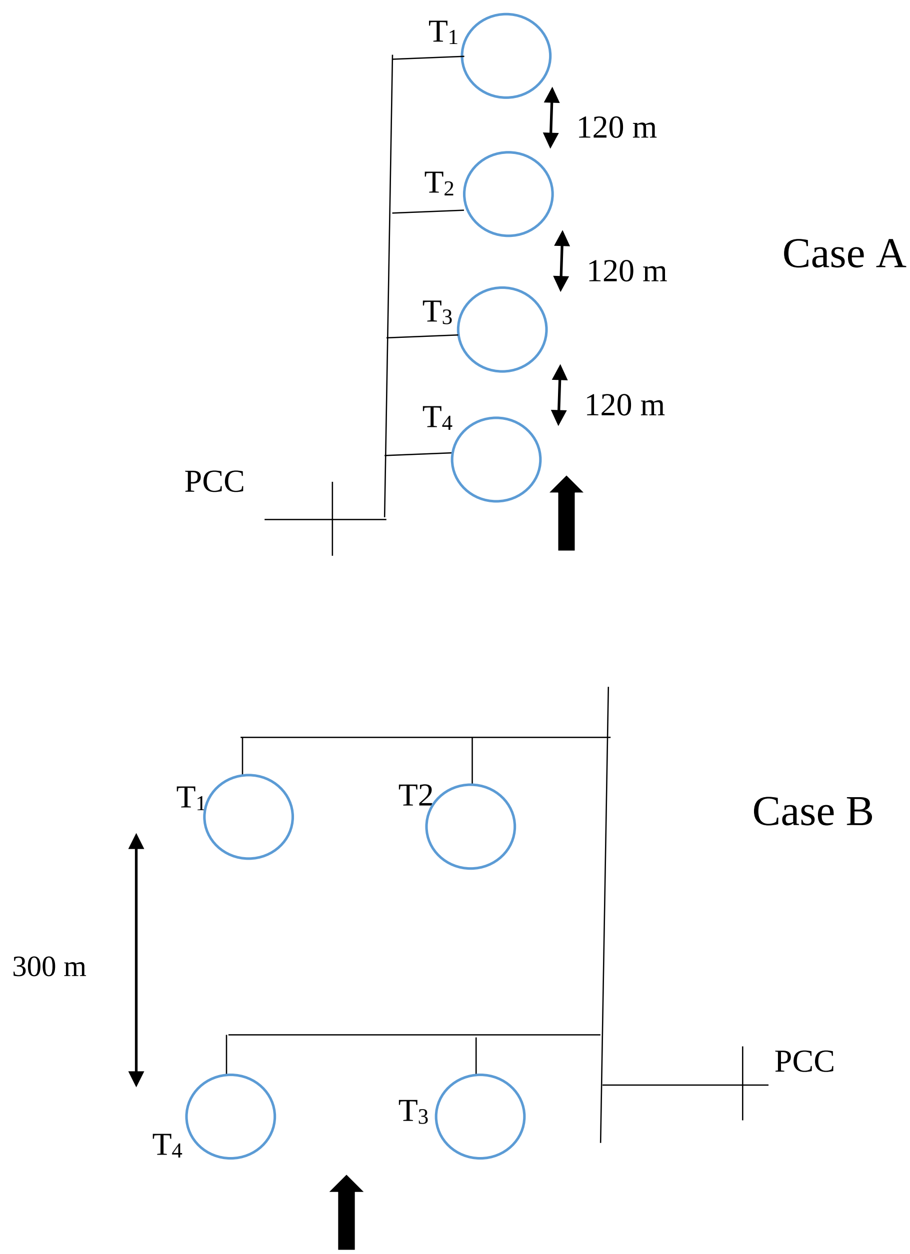

Figure 9 – Two layouts of 4 identical DFIGs is considered

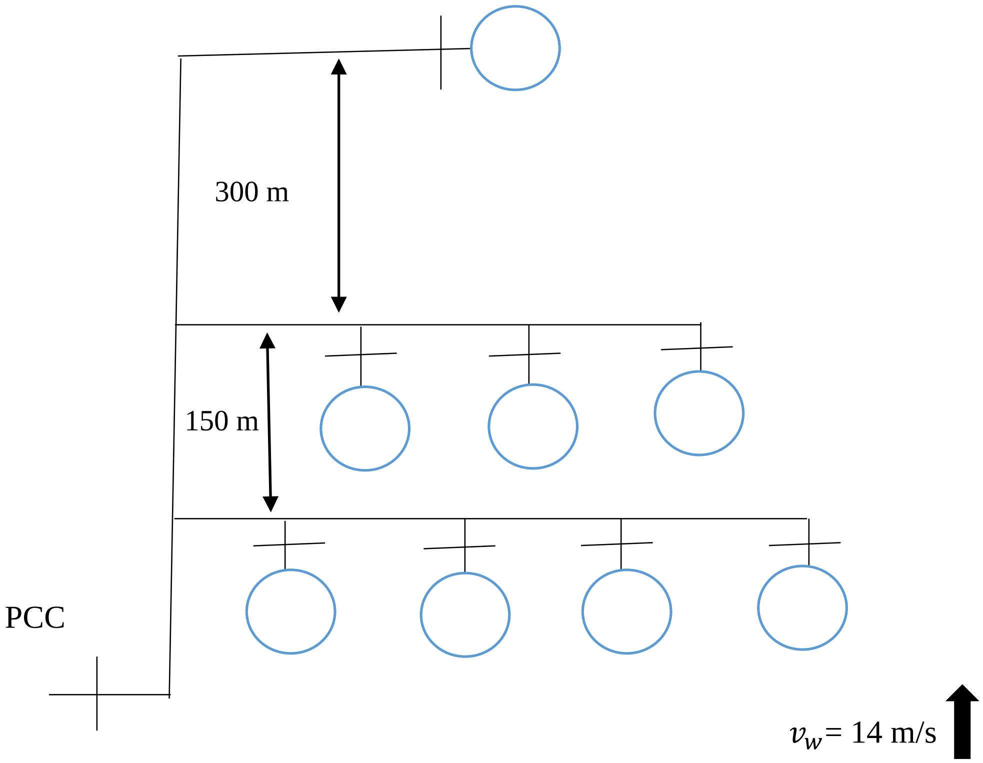

Figure 10- Case C

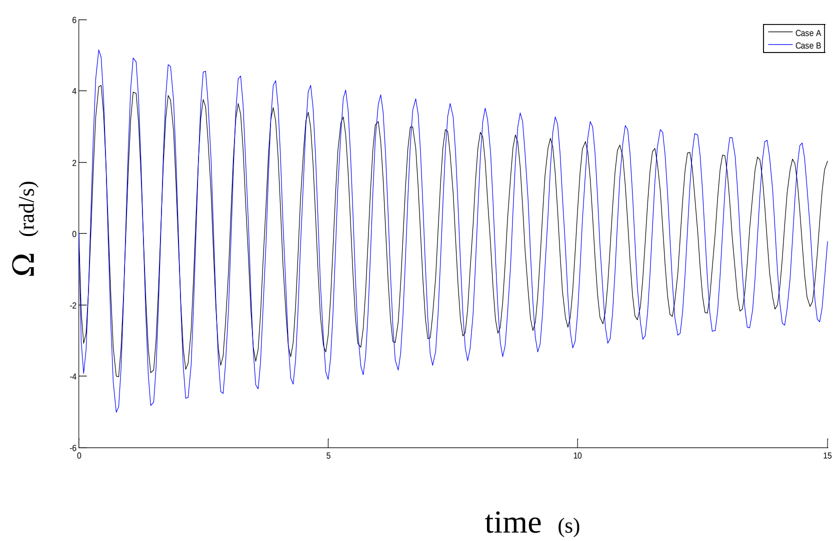

Figure 11 - SG speed for two cases mentioned in A and B

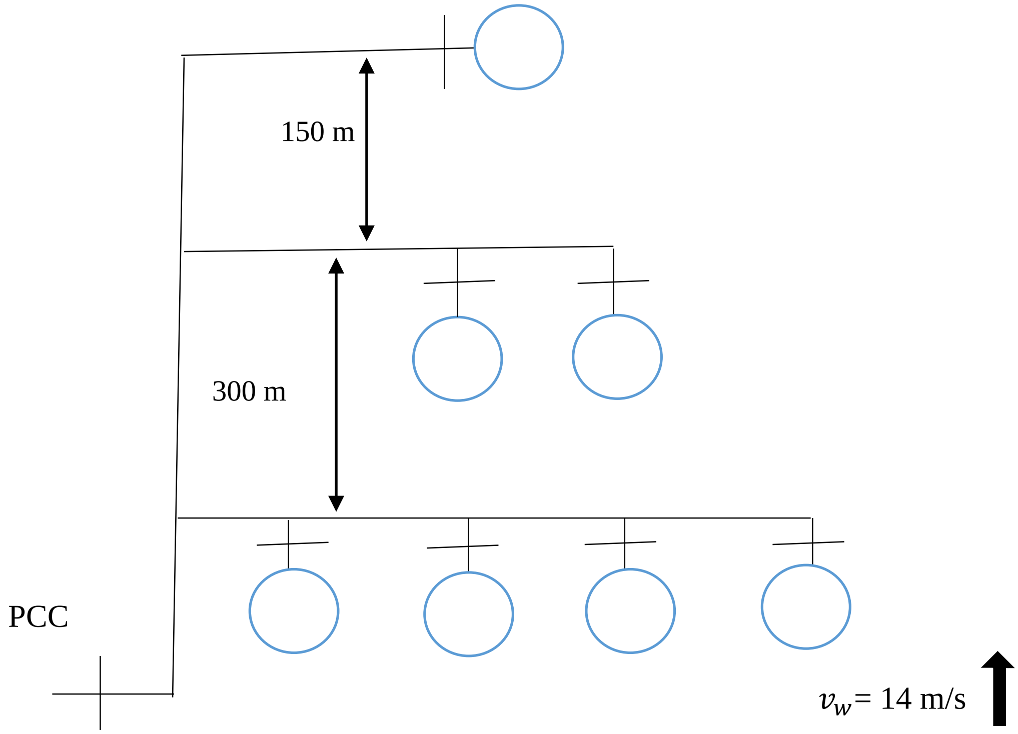

Figure 12- Case D

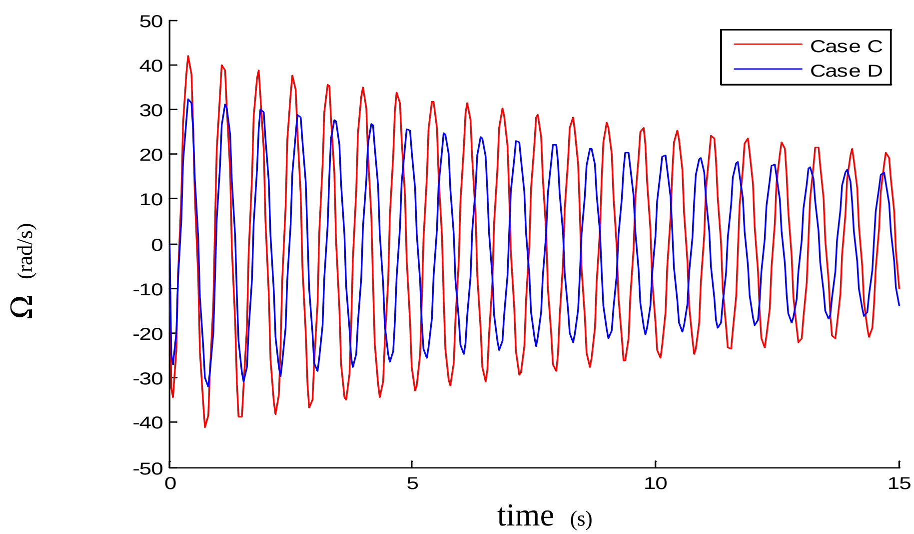

Figure 13- Comparison of cases C and D.

Table 3- Eigenvalue imaginary parts for the cases A, B, C and D.

Case	Eigenvalue imaginary part
A	7.73
B	7.44
C	8.75
D	8.59

CHAPTER 5

Conclusion and future work

Summary of the modeling and analysis is presented in this chapter.

Considering a wind turbine generator connected to a synchronous generator, it is observed that increasing generated wind power, results in a reduced frequency of SG rotor speed oscillations. With a constant change in wind speed, the amount of percent change in oscillations frequency is almost the same for different amounts of SG inertias.

In a wind farm connected power system, layout of the farm affects SG rotor speed dynamics. The system oscillations frequency reduces more as farm generators are spread further from the front row.

There is a need for understanding how the spatial location of the farms affect the overall system dynamics, and if the location factor worsens the dynamic response in any way. Designing location-dependent controllers to counteract the adverse impacts of DFIG integration will be a critical research task for future studies. Yet another important question that follows from the results of this research is how other fluid dynamical characteristics such as edge effects of the turbine towers affect the oscillation dynamics of the grid, studies on which requires detailed simulations on computational fluid dynamics. Our goal would be to use advanced CFD software codes to simulate the internal dynamics of wind farms and to test how their operating principles as well as their relationship to the placement of the turbines affect the power dynamics of the DFIGs and thereby the oscillation dynamics of the grid.

REFERENCES

[1] e. a. P. Bousseau, "Solutions for the grid integration of wind farms," *Wind Energy*, vol. 9, no. 1, 2006.

[2] "NREL," July 2008. [Online]. Available: http://www.nrel.gov/docs/fy08osti/41869.pdf. [Accessed 1 August 2013].

[3] R. R. P. K. K. P. P. V. E.Y. Bitar, "Bringing Wind Energy to Market," *IEEE Transactions on Power Systems* , vol. 27, no. 3, 2012.

[4] Y. Gu, J. McCalley and M. Ni, "Coordinating Large-Scale Wind Integration and Transmission Planning," *IEEE Transactions on Sustainable Energy,* vol. 3, no. 4, 2012.

[5] L. Ochoa, A. Padilha-Feltrin and G. Harrison, "Time-Series-Based Maximization of Distributed Wind Power Generation Integration," *IEEE Transactions on Energy Conversion,* vol. 23, no. 3, 2008.

[6] A. Srivastava and N. Schulz, "Impact of Distributed Generations with Energy," *IEEE Systems Journal,* vol. 6, no. 1, 2012.

[7] R. Al Abri, E. El-Saadany and Y. Atwa, "Optimal Placement and Sizing Method to Improve the Voltage Stability Margin in a Distribution System Using Distributed Generation," *IEEE TRANSACTIONS ON POWER SYSTEMS,* vol. 28, no. 1, 2012.

[8] M. Yin, X. Ge and Y. Zhang, "Major problems concerning China's large-scale wind power integration," in *Power and Energy Society General Meeting*, San Diego, CA, 2011.

[9] J. Slootweg and W. Kling, "Impacts of distributed generation on power system transient stability," in *Power Engineering Society Summer Meeting*, Chicago, IL, USA, 2002.

[10] J. Slootweg and W. Kling, "Aggregated modelling of wind parks in power system dynamics simulations," in *IEEE Power Tech Conference Proceedings*, Bologna, 2003.

[11] J. Slootweg, H. Polinder and W. Kling, "Dynamic modelling of a wind turbine with doubly fed induction generator," in *Power Engineering Society Summer Meeting*, Vancouver, BC, 2001.

[12] F. Hughes, O. Anaya-Lara, N. Jenkins and G. Strbac, "Control of DFIG-based wind generation for power network support," *IEEE transaction on power systems,* vol. 20, no. 4, 2005.

[13] J. Ekanayake, L. Holdsworth, X. Wu and N. Jenkins, "Dynamic modeling of doubly fed induction generator wind turbines," *IEEE transactions on power systems,* vol. 18, no. 2, 2003.

[14] L. Holdsworth, X. Wu, J. Ekanayake and N. Jenkins, "Direct solution method for initialising doubly-fed induction wind turbines in power system dynamic models," *Generation, Transmission and Distribution, IEE Proceedings* , vol. 150, no. 3, 2003.

[15] L. Fan, Z. Miao and D. Osborn, "Impact of doubly fed wind turbine generation on inter-area oscillation damping," in *Power and Energy Society General Meeting*, Pittsburgh, PA, 2008.

[16] E. Muljadi, C. Butterfield, B. Parsons and A. Ellis, "Grid, Effect of Variable Speed Wind Turbine Generator on Stability of a Weak," *IEEE transactions on power systems,* vol. 22, no. 1, 2007.

[17] H. Pulgar-Painemal and P. Sauer, "Power system modal analysis considering doubly-fed induction generators," in *Bulk Power System Dynamics and Control (iREP) - VIII (iREP), 2010 iREP Symposium* , Rome, 2011.

[18] B. Wu, Y. Lang, N. Zargari and S. Kouro, Power Conversion and Control of Wind Energy Systems, Wiley-IEEE Press , 2011.

[19] W. K. J.G. Slootweg, "The impact of large scale wind power generation on power system oscillations," *Electric Power Systems Research,* vol. 67, no. 1, 2003.

[20] E. F. E.-S. a. M. M. A. S. Tarek H. M. El-Fouly, "Impacts of Wake Effect and Time Delay on the Dynamic Analysis of Wind Farms Models," *Bulletin of Science Technology Society*, 2008.

[21] H. Kim, C. Singh and A. Sprintson, "Simulation and Estimation of Reliability in a Wind Farm Considering the Wake Effect," *Sustainable Energy, IEEE Transactions,* vol. 3, no. 2, 2012.

[22] X. Han, J. Guo, P. Wang and Y. Jia, "Adequacy study of wind farms considering reliability and wake effect of WTGs," in *Power and Energy Society General Meeting*, 2011.

[23] D. Gayme and A. Chakrabortty, "Impact of wind farm placement on inter-area oscillations in large power systems," in *American Control Conference (ACC),* Montreal, QC, 2012.

[24] O. A.-L. G. B. N. J. A. Shafiu, " Aggregated Wind Turbine Models for Power System Dynamic Studies," *Wind engineering,* vol. 30, no. 3, 2006.

[25] X. Han, J. Guo and P. Wang, "Adequacy study of a wind farm considering terrain and wake effect," *Generation, Transmission & Distribution, IET* , vol. 6, no. 10, 2012.

APPENDIX

Appendix: System Data

Controller parameters	kp1=1 kp2=1 kp3=1 ki1=5 ki2=5 ki3=5 ki4=5 kp4=1 Qref=0 C= $3.2397 \times 10^{-9}\ \ s^3/rad^3$
SG parameters	ω_s=120 π H=10 s
DFIG parameters	*Xm=3.5092 pu* *Xr=3.5859 pu* Xs=3.5 pu H_D=4 s Rs=.01015 pu Rr=.0088 pu
Network parameters	P_L=0.3 pu Q_L=.05 pu X_d =2 pu